

# Numerical modeling of a new integrated PV-TE cooling system and support

Giampietro Fabbri<sup>a</sup>, Matteo Greppi<sup>b,\*</sup>

<sup>a</sup> D.I.N., University of Bologna, Viale Risorgimento 2, 40136 Bologna, Italy

<sup>b</sup> D.E.I., University of Bologna, Viale Risorgimento, 2, 40136 Bologna, Italy



## ARTICLE INFO

### Keywords:

Solar panels  
Cooling  
Integration  
Photo-thermoelectric  
Structural function

## ABSTRACT

In this article, an innovative cooling system for photovoltaic panels is presented. This system uses the Seebeck effect to generate electricity. The proposed device differs from existing photothermoelectric systems by means of a compact, efficient and space-saving apparatus.

In fact, in the proposed device the thermoelectric generator is integrated in the heat exchange system since the thermoelectric effect takes place inside the heat exchanger and only a small part of the removed heat is used to create the required temperature difference. A preliminary numerical analysis of the thermoelectric behaviour of the proposed device under different geometrical and fluid-dynamic conditions is also presented. For a standard photovoltaic panel of  $100 \times 125$  cm the proposed cooling system allows an increase of almost 15% of the electrical power converted by the cells. Moreover, the exploited Seebeck effect provides an electrical power (ranging from 61.2 to 71.2 W in the studied cases) that is respectively 10.9 and 1.33 times the power required for forced ventilation. The maximum system electrical power reachable, using commercial inorganic thermoelectric materials, considering all electrical power gains and losses is next to 300–310 W/m<sup>2</sup>.

## 1. Introduction

Over the last decade, several techniques have been studied to increase the conversion efficiency of solar panels. The energy converted by photovoltaic cells can be increased by keeping their surface temperature at a low value. Various cooling systems have been designed for this purpose. Some of them disperse the heat removed by the cells into the environment [1,2], others transfer it to a heat transfer fluid (usually water) which makes it available for different uses [3–8]. However, in many applications the thermal power removed by the photovoltaic cells is not directly exploitable and it is more convenient to disperse it into the environment, since the only energy required is electrical one. In these cases, the conversion efficiency can be increased by exploiting thermoelectric effects. In particular, several systems have been designed which exploit Peltier or Seebeck effects. Chein [9] focused on applications of the thermoelectric cooler (TEC) in electronic cooling. The temperature of the cold side ( $T_c$ ) and the temperature difference between the cold and hot sides of the TEC ( $\Delta T = T_h - T_c$ ,  $T_h$  = temperature of the hot side of the TEC) were used as parameters. The results indicated that the cooling capacity could be increased by increasing  $T_c$  and decreasing  $\Delta T$ . Zhang [10] conducted a performance analysis study of the thermoelectric cooler (TEC) for high-power electronic packages such as processors. The results

of the analysis show that significant thermal improvements can be achieved based on optimised currents and cooling configurations. Pourkiaei [11] and Zhao [12] presented reviews on the state of the art and future applications for thermoelectric cooling devices and thermoelectric generators focusing on the growing interest in TEC technology. Shittu's review [13] on solar photovoltaic cooling and TEC integration emphasises that the combination of photovoltaic and thermoelectric generators would allow the use of a wider solar spectrum and provide higher performance, but the integration of both systems is complex due to their opposing characteristics. In photovoltaic panels cooled by systems exploiting the Seebeck effect (as described by Teffah [14] and Shittu [15]), the thermoelectric cooler (TEC) is usually placed between the cells and a finned heat sink (Fig. 1a). In this way, all the heat removed passes through the TEC, causing a temperature drop between the cells and the heat sink. Therefore, the lower the temperature drop, the better the efficiency of the photovoltaic cell, but conversely, the lower the efficiency of the TE. Enescu's review [16] concludes that the integration of the TEC device with PV cells can have two positive consequences: improving the power capacity of PV modules and increasing the electrical efficiency of the PV system. The transient power generation and efficiency of a CPV-TEC hybrid system was studied by Mahmoudinezhad [17]. The results showed that with increasing solar radiation, the power generation from CPV and TEC increased. Kiflemariam [18] numerically analyses the

\* Corresponding author.

E-mail address: [matteo.greppi2@unibo.it](mailto:matteo.greppi2@unibo.it) (M. Greppi).

**Nomenclature description**

$L_t$	Total length
$W_t$	Total width
$H_t$	Total height
$d_a$	Aluminum sheet thickness
$L_l$	Leg cross section in length
$H_l$	Leg height
$p$	Pitch
$n_l$	Number of legs in length
$n_w$	Number of legs in width
$L_n$	Length of legs network
$W_n$	Width of legs network
$N_t$	Number of thermocouples
$M$	Module Rows
$T_{ref}$	Hot side cell temperature
$S_r$	Sensitivity ratio
$u$	Inlet velocity
$q$	Heat flux
$P_v$	Ventilation power
$P_e$	Thermoelectric power

performance of the not fully integrated thermoelectric-thermophotovoltaic (TEC-PVT) system. It is realised that having a higher concentration ratio results in higher energy production, while increasing the heat transfer coefficient by convection between the external surfaces and the atmosphere and lowering thermal resistance between the photovoltaic cells and the TEG, helps to keep the temperature of the PV at an optimal level. Li [19] studies the optimal thermoelectric geometry to achieve a good performance for a photovoltaic thermoelectric device (PV-TEC) and a solar thermoelectric generator (STEC) obtaining that the best thermoelectric geometry in a hybrid PV-TEC device depends on the type of PV cell and this is different from that of STEC under the same conditions. The latest research on heat sink-cooled PV-TEC systems has confirmed an increase in electrical efficiency over the same area, but low thermal efficiency and high installation and operating costs. All recent research and market solutions [20–24] present separate heat exchangers and thermoelectric generators and the heat removed from the photovoltaic cells passes entirely through the thermocouples. This leads to a reduction in the exchange efficiency (if a high temperature difference between the thermocouples is designed) and a reduction in the Seebeck effect (if a low temperature drop in the thermocouples is designed). Alternative solutions also present cooling systems for a photovoltaic panel comprising a plurality of Peltier cells having a first face in contact with the photovoltaic cells and a second face in contact with a heat exchanger (in this case, fins), which exchanges heat with a fluid. Such systems require electrical connections to be made by cable. Furthermore, since they consist of a first layer of Peltier cells and a second layer of cooling fins, they are very costly, heavy and bulky.

## 2. The innovative cooling system

In this paper we propose an innovative cooling system (Fig. 1b), that allows on the technical and production side a significant simplification of the solar cell cooling and thermoelectric conversion technology using the Seebeck effect by integrating the heat exchanger with the thermoelectric

converter. The heat exchanger also acts as a support for the cells. The main innovative aspects of our technology therefore concern the integration between the heat exchanger and the thermoelectric generator, the independence between heat exchange efficiency and thermoelectric generation efficiency, because only part of the heat removed from the panel passes through the thermocouples, and the use of a system of joints to make the electrical contacts with a consequent simplification of construction and installation. In addition, the apparatus can be made according to a modular structure so that it can be easily adapted to different sizes of photovoltaic panel. Finally, the patented apparatus, besides being useful for cooling the solar panel and increasing its efficiency, also has the advantage, when mounted on the roof, of acting as a thermal insulator for the roof itself. The core of the TEC/heat sink module consists of P and N doped thermoelectric legs joined together by means of pressure joints, in order to construct thermocouples that are more compact and easier to build and assemble. In addition, the integrated TEC cooling system acts as a support for the solar panel. It also adapts to different needs thanks to its modularity.

In the following, the TEC cooling system is described in detail and a preliminary numerical analysis of its thermoelectric behaviour is presented.

## 3. Integrated TEG apparatus

The integrated module (Fig. 1-b) consists of a sandwich between two thick aluminium sheets of thickness  $d_a$  and a TEC core. The PV side foil is coated on the bottom aluminium surface with a layer of elastic electrical insulation material with high thermal conductivity. The plate on the opposite side is coated on the upper surface with the same thermally conductive and electro-insulating elastic material. The external module dimensions are  $L_t \times W_t \times H_t$ . The legs network dimensions are  $L_n \times W_n$  with the pitch  $p$  defined as the space between P and N type doped legs surfaces. A series of  $M$  row of couple of legs in length and  $N_t$  columns of couple of legs in width makes up the TEC module core composed of  $M \times N_t$  thermocouples, being each couple of legs of two different conductive or semiconductive materials. The thermoelectric materials are joined together by means of pressure joints. For this analysis we consider commercial inorganic thermoelectric materials of P and N types semiconductors such as  $\text{Bi}_2\text{Te}_3$  (Bismuth Telluride) and  $\text{PbTe}$  (Lead Telluride).

## 4. Numerical model

A finite steady-state model was developed to numerically simulate the performance of the integrated PVTE module, bounded by the inlet and outlet faces and the thermally insulated ones (Fig. 3). Let  $L_t$  be the distance between the inlet and outlet planes in the  $y$  direction,  $W_t$  the distance between the side planes in the  $x$  direction and  $H_t$  the height of the simulated module. The section of the domain studied in the planes normal to the  $x$  and  $y$  axes is shown in Fig. 2. The numerical boundaries adopted are the pressure inlet and outlet velocities, the insulation at the side walls and the bottom surface, the heat flux equal to 800 W at the front surface (Fig. 3). The governing equations that analyse the behaviour of the integrated thermoelectric and fluid dynamic device are the equations of continuity (1), momentum (2), heat flow (3) and continuity of electric charge (4):

$$\frac{\partial \rho}{\partial t} + \frac{\partial(\rho u)}{\partial y} = 0 \quad (1)$$

$$\frac{\partial^2 u}{\partial y^2} + \frac{\partial^2 u}{\partial x^2} = \frac{1}{\mu} \left( \frac{\partial p}{\partial y} + \frac{\partial p}{\partial x} \right) \quad (2)$$

$$\rho C \left( \frac{\partial T}{\partial t} \right) + \vec{\nabla} \cdot \vec{q} = Q_t \quad (3)$$

$$\vec{\nabla} \cdot \left( \epsilon \frac{\partial \vec{E}}{\partial t} \right) + \vec{\nabla} \cdot \vec{J} = Q_e \quad (4)$$

where  $\rho$  is the fluid density,  $\mu$  is the dynamic viscosity,  $u$  is the fluid velocity,  $p$  is the generalised pressure,  $T$  is the temperature,  $E$  is the electric field,  $q$  is the heat flow,  $J$  is the electric current density,  $Q_t$  is the internal heat generator,  $Q_e$  is the electric charge,  $C$  is the heat capacity and  $\epsilon$  is the electric permittivity. The current density  $J$  (6) is generated by a coupling of reversible Seebeck effect and irreversible Joule effect:

$$\vec{J} = \sigma \vec{E} - \sigma S \vec{\nabla} T \quad (5)$$

The heat flux  $q$  is generated by couple effect of reversible Peltier and irreversible Fourier effect:

$$\vec{q} = \pi \vec{J} - k \vec{\nabla} T \quad (6)$$

where  $\pi$  is the Peltier coefficient,  $k$  is the thermal conductivity,  $\sigma$  is the electrical conductivity and  $S = V/\Delta T$  is the Seebeck coefficient ( $V$  is the electric potential). The electric field can be derived from the scalar electric potential  $\phi$  as:

$$\vec{E} = - \vec{\nabla} \phi \quad (7)$$

### 5. Results

A wide range of geometrical parameters ( $L_l$ ,  $W_l$  and  $p$ ) in the defined analysis intervals was numerically studied for the proposed device. Due to technical and operational production limitations, the final choice could be made on higher values of leg width and length. The parameters

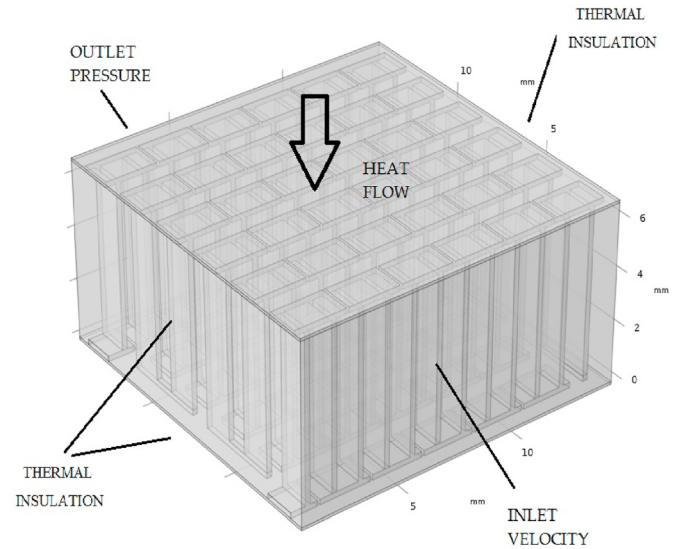


Fig. 3. Boundary conditions.

of a reference geometry for a module of  $1.4 \times 1.4$  cm are given in Table 1. Fig. 4 a-b, 5 a-b and 6 a-b show the velocity, temperature and pressure distributions obtained for inlet cross-flow velocities ( $u$ ) equal to 1 and 3 m/s and heat flux applied to the upper surface equal to  $0.1568 \text{ W}$  corresponding to  $800 \text{ W/m}^2$  (irradiance on PV cell surface).

For the geometry considered, the difference between the temperature of the cooled surface and that of the incoming air is  $50.45 \text{ }^\circ\text{C}$  ( $u = 1 \text{ m/s}$ ) and  $48.7 \text{ }^\circ\text{C}$  ( $u = 3 \text{ m/s}$ ), while the electrical potential difference obtained is  $0.46 \text{ V}$  ( $u = 1 \text{ m/s}$ ) and  $0.52 \text{ V}$  ( $u = 3 \text{ m/s}$ ). The pumping power

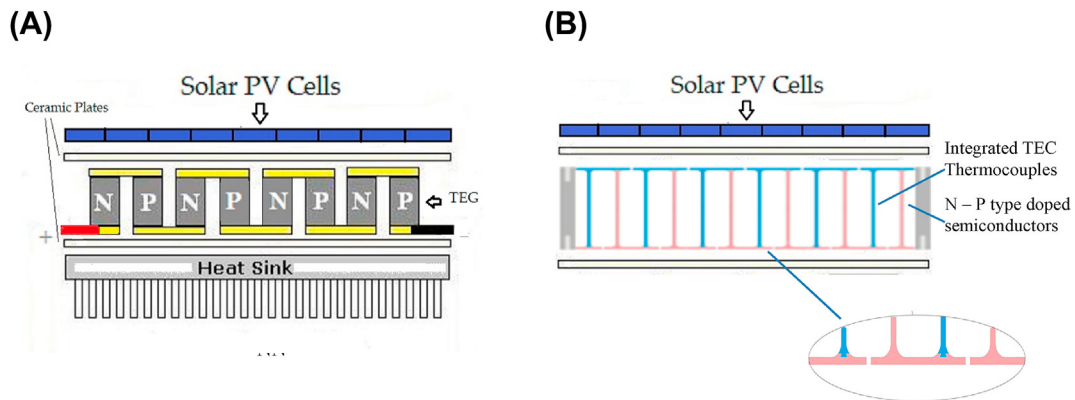


Fig. 1. a State of the art PV-TEG module b Integrated apparatus.

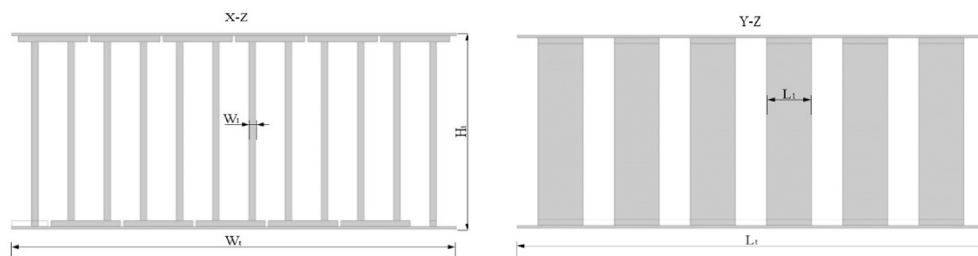


Fig. 2. Integrated module section views (X-Z, Y-Z).

**Table 1**  
List of parameters.

Parameters	Value	Unit
$L_t$	14.1	mm
$W_t$	14.1	mm
$H_t$	7	mm
$d_a$	0.3	mm
$H_1$	6.2	mm
$n_1$	6	-
$n_W$	12	-
$L_n$	12.5	mm
$W_n$	12.8	mm
$Q$	800	W/m <sup>2</sup>
$L_l$	0.75	mm
$W_1$	0.15	mm
$p$	0.8	mm

$P_v$  required to move the air is 0.001092 W ( $u = 1$  m/s) and 0.0105 W ( $u = 3$  m/s). It has been calculated as  $P_v = dP \cdot u \cdot A$ ,  $dP$  being the pressure drop on the module,  $u$  the velocity, and  $A$  the area of the section. The electrical output power of the module  $P_e$  is 0.012 W ( $u = 1$  m/s) and 0.014 W ( $u = 3$  m/s). It was calculated as  $P_e = V \cdot I$ ,  $V$  being the electrical

potential of the module and  $I = J \cdot A$  being the current for a single TEG element relative to the two semiconductors,  $J$  being the current density and  $A$  being the cross-sectional area. In order to evaluate the influence of the geometrical parameters on the device performance, some geometry variations with respect to the reference case have been considered. Fig. 7a-b-c and Fig. 8 a-b-c show the electric potential difference obtained numerically between the ends of the TEG module by varying the geometrical parameters  $L_l$ ,  $W_1$  and  $p$  for input speeds of 1 and 3 m/s. The values of the parameters are given in Table 2.

It is evident that by increasing  $L_l$ , the potential difference decreases. Furthermore, by increasing  $W_1$  the potential difference decreases, while by decreasing  $p$  the potential difference increases.

Fig. 9 shows a comparison between the electrical power converted by PV cells without a cooling system (only natural convection from the top and side surfaces) and with the integrated cooling system.

An innovative thermocouple (Fig. 10) based on a new polymeric thermoelectric material (PEDOT) has been under simulated ( $u = 3$  m/s;  $p = 0,8$  mm):

The reliability of the numerical results obtained was then assessed by means of a sensitivity analysis (Fig. 11). As the mesh was progressively refined (Table 3), we discontinued the procedure when no significant differences were assessed on the reference output parameter (potential difference).

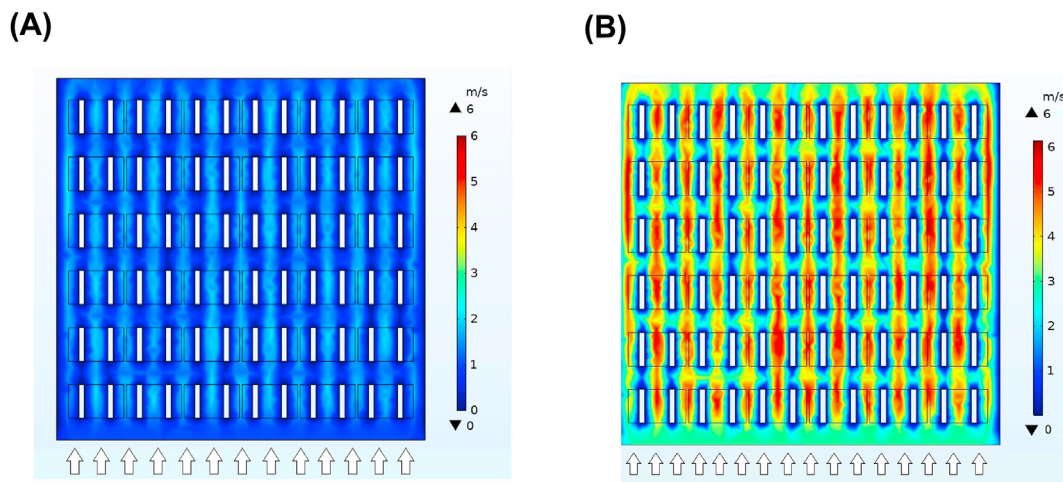


Fig. 4. a 2D x-y velocity distribution ( $u = 1$  m/s) b 2D x-y velocity distribution ( $u = 3$  m/s).

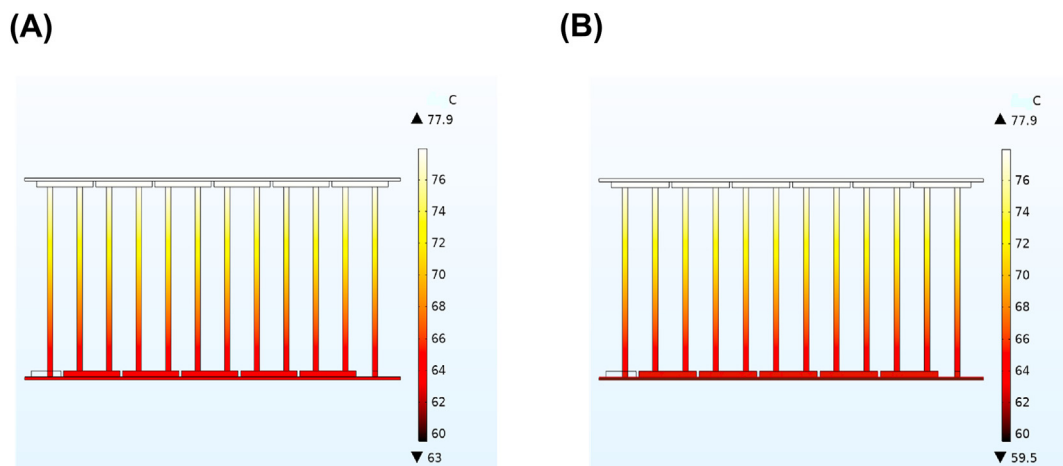


Fig. 5. a 2D x-z temperature distribution ( $u = 1$  m/s) b 2D x-z temperature distribution ( $u = 3$  m/s).

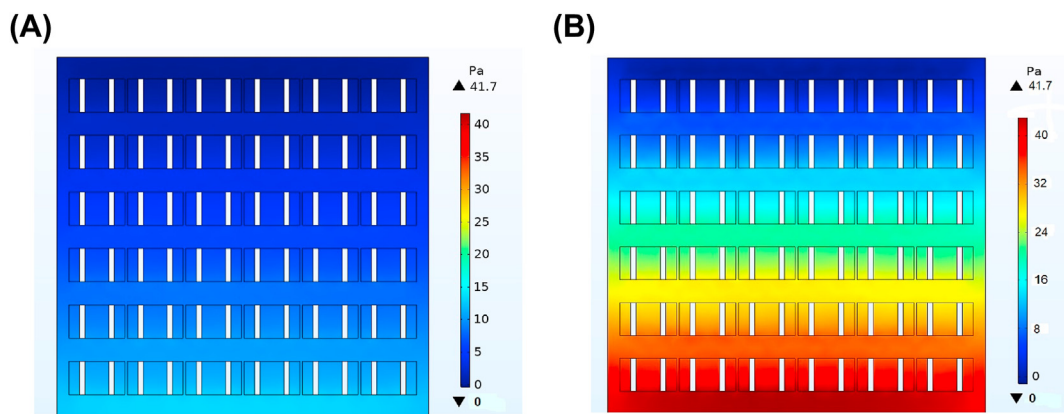


Fig. 6. a 2D x-y pressure distribution ( $u = 1$  m/s) . b 2D x-y pressure distribution ( $u = 3$  m/s).

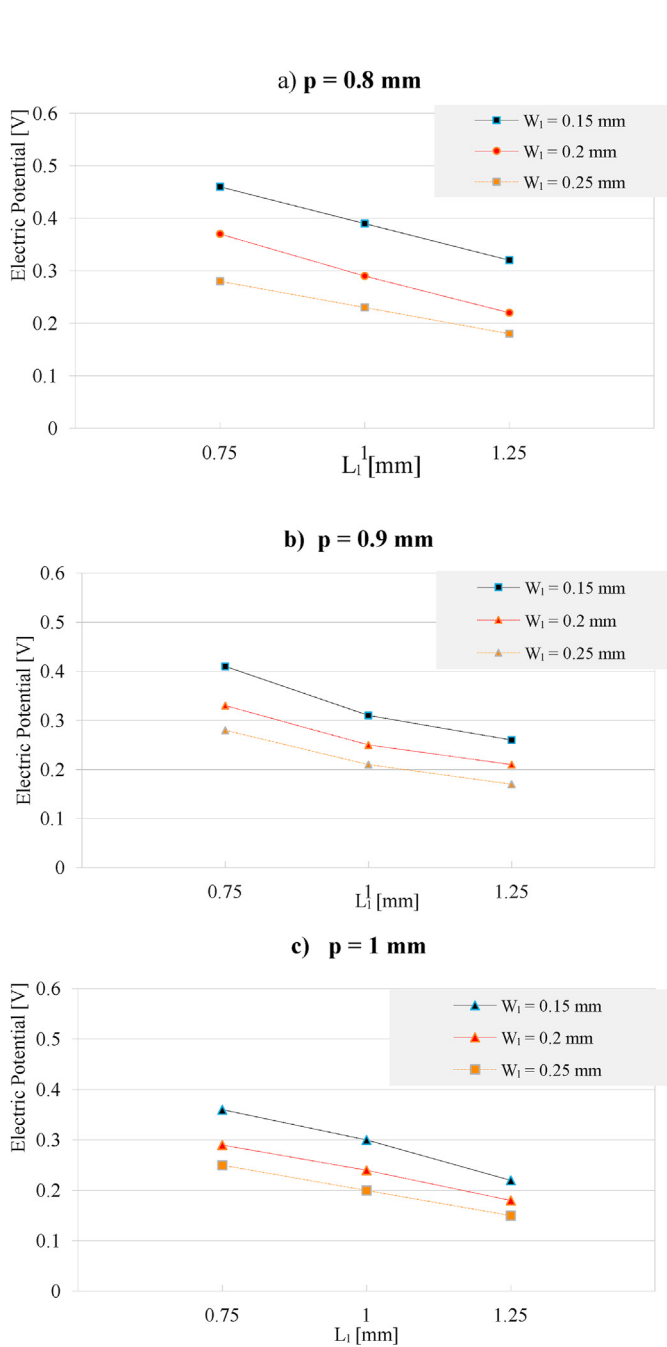


Fig. 7. a-b-c Electric potential distribution ( $u = 1$  m/s).

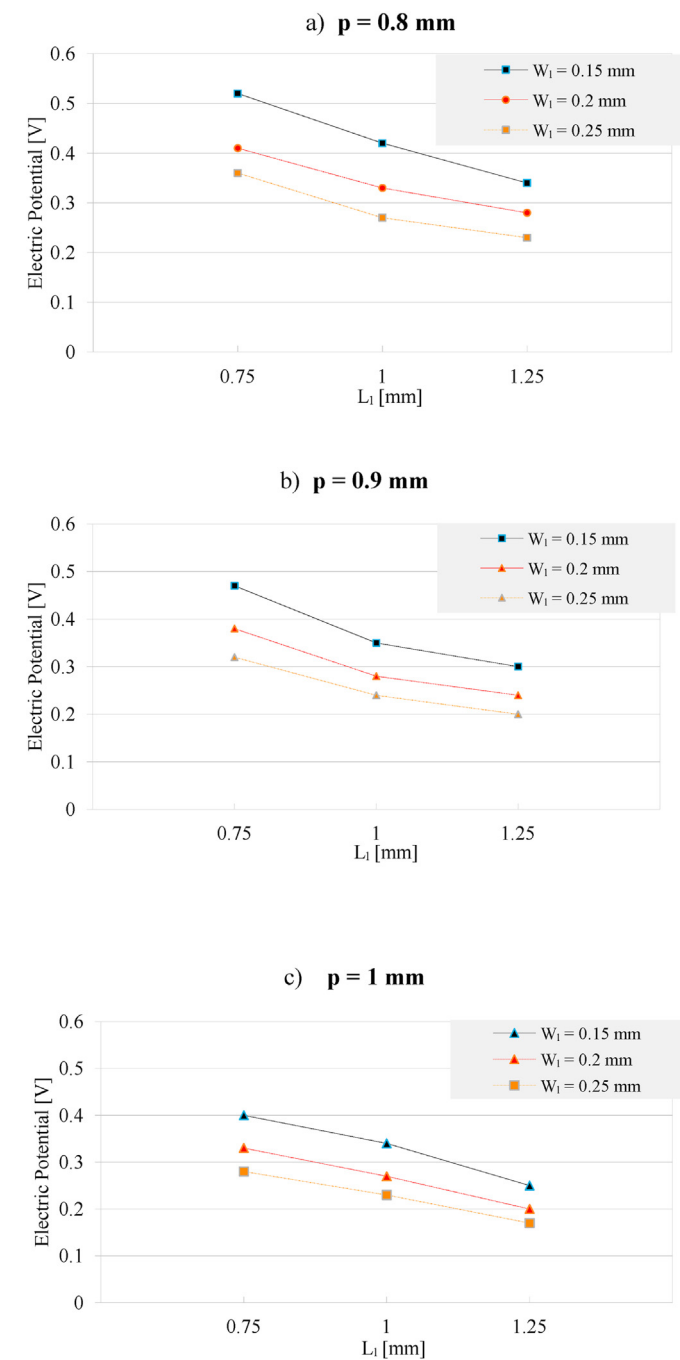


Fig. 8. a-b-c Electric potential distribution ( $u = 3$  m/s).



**Table 2**  
Geometrical parameters.

$L_1$ $W_1$	0.00075	0.001	0.00125
a) $p = 0.8$ mm ( $N_t$ "columns", $M$ "rows")			
0.00015	$N_t = 12; M = 6$	$N_t = 12; M = 5$	$N_t = 12; M = 4$
0.0002	$N_t = 11; M = 6$	$N_t = 11; M = 5$	$N_t = 11; M = 4$
0.00025	$N_t = 11; M = 6$	$N_t = 11; M = 5$	$N_t = 11; M = 4$
b) $p = 0.9$ mm ( $N_t$ "columns", $M$ "rows")			
0.00015	$N_t = 11; M = 6$	$N_t = 11; M = 5$	$N_t = 11; M = 4$
0.0002	$N_t = 10; M = 6$	$N_t = 10; M = 5$	$N_t = 10; M = 4$
0.00025	$N_t = 10; M = 6$	$N_t = 10; M = 5$	$N_t = 10; M = 4$
c) $p = 1$ mm ( $N$ "columns", $R$ "rows")			
0.00015	$N_t = 10; M = 6$	$N_t = 10; M = 5$	$N_t = 10; M = 4$
0.0002	$N_t = 10; M = 6$	$N_t = 10; M = 5$	$N_t = 10; M = 4$
0.00025	$N_t = 10; M = 6$	$N_t = 10; M = 5$	$N_t = 10; M = 4$

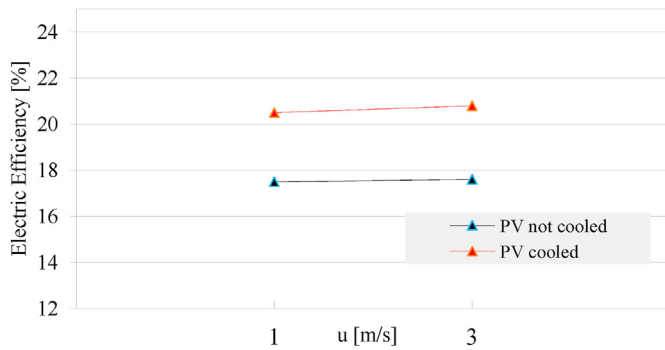


Fig. 9. Electric efficiency (PV panel).

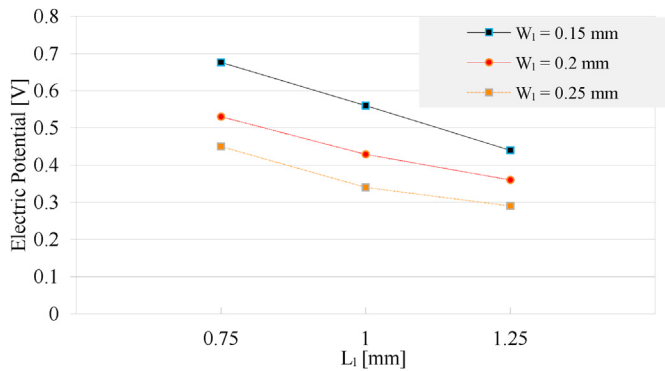


Fig. 10. Electric potential distribution (PEDOT).

**Table 3**  
Mesh parameters.

	Mesh 1 (Size) [mm]	Mesh 2 (Size) [mm]	Mesh 3 (Size) [mm]	Mesh 4 (Size) [mm]	Mesh 5 (Size) [mm]
Max element dimension	1.42	1.08	0.743	0.511	0.292
Min element dimension	0.255	0.135	0.054	0.0219	0.00287
Max growth ratio	1.5	1.45	1.4	1.35	1.3

**6. Conclusions**

In this work, a modular cooling system for photovoltaic panels has been proposed, which also increases the electrical power output by exploiting the Seebeck effect. A reference configuration of the geometrical parameters of the cooling system suitable for practical applications was identified, with respect to which the effect of changing certain parameters was investigated. For a standard photovoltaic panel of  $100 \times 125$  cm (i.e.  $7 \times 9$  modules) the proposed cooling system allows an increase of almost 15% of the electrical power converted by the cells (Fig. 9). Moreover, the exploited Seebeck effect provides an electrical power (ranging from 61.2 to 71.2 W in the studied cases) that is respectively 10.9 and 1.33 times the power required for forced ventilation. The best analysed operating choice is  $u = 1$  m/s. The maximum system electrical power reachable, for inorganic commercial thermoelectric materials, considering all electrical power gains and losses is near to  $300\text{--}310$  W/m<sup>2</sup>.

The results presented were obtained considering materials such as

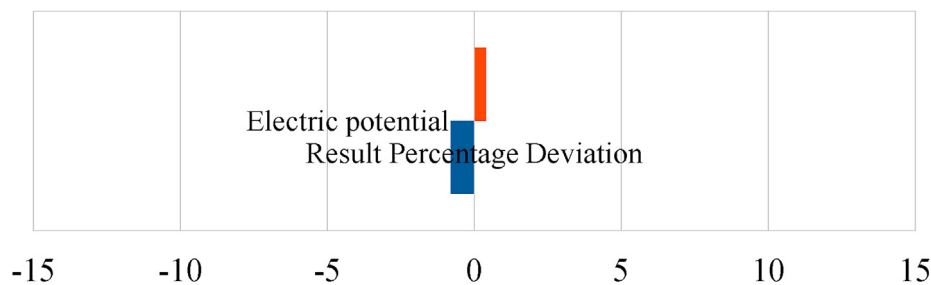


Fig. 11. Mesh sensitivity analysis.

Bi<sub>2</sub>Te<sub>3</sub> (Bismuth Telluride) and PbTe (Lead Telluride), which are currently used in thermoelectric generators. Greater increases in photovoltaic panel performance will be achieved with the proposed modular cooling system, which uses thermocouples made from innovative materials that are now being studied. Thermocouples made from nano-doped organic materials (despite some technical production limitations to be fixed), due to a higher ZT (figure of merit) value, could not only provide increases of up to 15% in the electrical power converted by photovoltaic cells but also thermoelectrically generate up to 100 W for a standard 250 W photovoltaic panel (Fig. 10).

#### Credit author statement

Greppi Matteo: Conceptualization, Methodology, Data curation, Writing Original draft preparation, Visualization, Investigation, Fabbri Giampietro: Conceptualization, Supervision, Validation, Writing Original draft preparation, Reviewing and Editing.

#### Declaration of competing interest

The authors declare that they have no known competing financial interests or personal relationships that could have appeared to influence the work reported in this paper.

#### References

- [1] A. Yesilyurt, M. Nasiri, A. Ozakin, Techniques for enhancing and maintain electrical efficiency of photovoltaic systems, *Int. J. New Technol. Res.* 4 (4) (2018) 44–53. ISSN:2454-4116.
- [2] Mohamed R. Goma, Waleed Hammad, Mujahed Al-Dhaifallah, Hegazy Rezk, Performance enhancement of grid-tied PV system through proposed design cooling techniques: an experimental study and comparative analysis, *Sol. Energy* 211 (2020) 1110–1127, <https://doi.org/10.1016/j.solener.2020.10.062>. ISSN 0038-092X.
- [3] Y. Vorobiev, J. González-Hernández, P. Vorobiev, L. Bulat, Thermal-photovoltaic solar hybrid system for efficient solar energy conversion, *Sol. Energy* 80 (2006) 170–176, <https://doi.org/10.1016/j.solener.2005.04.022>.
- [4] Lebbi Mohamed, Khaled Touafek, Benchatti Ahmed, Lyes Boutina, Abdelkrim Khelifa, Mohamed Taher Baissi, Samir Hassani, Energy performance improvement of a new hybrid PV/T Bi-fluid system using active cooling and self-cleaning: experimental study, *Appl. Therm. Eng.* 182 (2021) 116033, <https://doi.org/10.1016/j.applthermaleng.2020.116033>. ISSN 1359-4311.
- [5] S. Kianifard, M. Zamen, A. Abbas Nejad, Modeling, designing and fabrication of a novel PV/T cooling system using half pipe, *J. Clean. Prod.* 253 (2020) 119972, <https://doi.org/10.1016/j.jclepro.2020.119972>. ISSN 0959-6526.
- [6] Shuang-Ying Wu, Chen Chen, Lan Xiao, Heat transfer characteristics and performance evaluation of water-cooled PV/T system with cooling channel above PV panel, *Renew. Energy* 125 (2018) 936–946, <https://doi.org/10.1016/j.renene.2018.03.023>. ISSN 0960-1481.
- [7] Tareq Salameh, Muhammad Tawalbeh, Adel Juaidi, Ramez Abdallah, Abdulkadir Hamid, A novel three-dimensional numerical model for PV/T water system in hot climate region, *Renew. Energy* 164 (2021) 1320–1333, <https://doi.org/10.1016/j.renene.2020.10.137>. ISSN 0960-1481.
- [8] R. Nasrin, N.A. Rahim, H. Fayaz, M. Hasanuzzaman, Water/MWCNT nanofluid based cooling system of PVT: experimental and numerical research, *Renew. Energy* 121 (2018) 286–300, <https://doi.org/10.1016/j.renene.2018.01.014>. ISSN 0960-1481.
- [9] R. Chein, G. Huang, Thermoelectric cooler application in electronic cooling, *Appl. Therm. Eng.* 24 (Issues 14–15) (October 2004) 2207–2217, <https://doi.org/10.1016/j.applthermaleng.2004.03.001>.
- [10] H.Y. Zhang, Y.C. Mui, M. Tarin, Analysis of thermoelectric cooler performance for high power electronic packages, *Appl. Therm. Eng.* 30 (2010) 561–568, <https://doi.org/10.1016/j.applthermaleng.2009.10.020>.
- [11] S. Pourkiaei, Thermoelectric Cooler and Thermoelectric Generator Devices: A Review of Present and Potential Applications, Modeling and Materials, *ume* 186, 2019, p. 115849, <https://doi.org/10.1016/j.energy.2019.07.179>, 1 November.
- [12] D. Zhao, G. Tan, A review of thermoelectric cooling: materials, modeling and applications, *Appl. Therm. Eng.* 66 (Issues 1–2) (May 2014) 15–24, <https://doi.org/10.1016/j.applthermaleng.2014.01.074>.
- [13] Khaled Teffah, Youtong Zhang, Xiao-long Mou, "Modeling and experimentation of new thermoelectric cooler–thermoelectric generator module", *International Communications in Heat and Mass Transfer*, *Energies* 11 (2018) 576, <https://doi.org/10.3390/en11030576>.
- [14] Shittu, et al., Comprehensive study and optimization of concentrated photovoltaic-thermoelectric considering all contact resistances, *Energy Convers. Manag.* 205 (2020) 112422, <https://doi.org/10.1016/j.enconman.2019.112422>.
- [15] D. Enescu, et al., Applications of hybrid photovoltaic modules with thermoelectric cooling, in: 8th International Conference on Sustainability in Energy and Buildings, SEB-16, Turin, Italy, 2016, <https://doi.org/10.1016/j.egypro.2017.03.253>.
- [16] Sajjad Mahmoudinezhad, Shaowei Qing, Alireza Rezaniakolaei, Lasse Aistrup Rosendahl, Transient model of hybrid concentrated photovoltaic with thermoelectric generator energy conversion and management, in: 9th International Conference on Applied Energy, ICAE2017, 2017, <https://doi.org/10.1016/j.egypro.2017.12.088>. Cardiff, UK.
- [17] R.Kiflemariam et al., Modeling integrated thermoelectric generator-photovoltaic thermal (TEG-PVT) system, *Proceedings from the 2011 Comsol Conference in Boston*.
- [18] Li, et al., Comparative analysis of thermoelectric elements optimum geometry between photovoltaic-thermoelectric and solar thermoelectric, *Energy* 171 (2019), <https://doi.org/10.1016/j.enconman.2019.112422>.
- [19] Birol Kılıç, Development of a composite PVT panel with PCM embodiment, TEG modules, flat-plate solar collector, and thermally pulsing heat pipes, *Sol. Energy* 200 (2020) 89–107, <https://doi.org/10.1016/j.solener.2019.10.075>. ISSN 0038-092X.
- [20] Heng Zhang, Yue Han, Jiguang Huang, Kai Liang, Haiping Chen, Experimental studies on a low concentrating photovoltaic/thermal (LCPV/T) collector with a thermoelectric generator (TEG) module, *Renew. Energy* 171 (2021) 1026–1040, <https://doi.org/10.1016/j.renene.2021.02.133>. ISSN 0960-1481.
- [21] R. Bjørk, K.K. Nielsen, The performance of a combined solar photovoltaic (PV) and thermoelectric generator (TEG) system, *Sol. Energy* 120 (2015) 187–194, <https://doi.org/10.1016/j.solener.2015.07.035>. ISSN 0038-092X.
- [22] G. Li, X. Chen, Y. Jin, Analysis of the primary constraint conditions of an efficient photovoltaic-thermoelectric hybrid system, *Energies* 10 (2017) 20, <https://doi.org/10.3390/en10010020>.
- [23] K.T. Park, S.M. Shin, A. Tazebay, et al., Lossless hybridization between photovoltaic and thermoelectric devices, *Sci. Rep.* 3 (2013) 2123, <https://doi.org/10.1038/srep02123>.